

Rotational disruption of dust grains by mechanical torques for high-velocity gas-grain collisions

THIEM HOANG,^{1,2} HYESEUNG LEE,³

¹*Korea Astronomy and Space Science Institute, Daejeon 34055, Republic of Korea; thiemhoang@kasi.re.kr*

²*University of Science and Technology, Korea, (UST), 217 Gajeong-ro Yuseong-gu, Daejeon 34113, Republic of Korea*

³*Korea Astronomy and Space Science Institute, Daejeon 34055, Republic of Korea*

ABSTRACT

Dust grains moving at hypersonic velocities of $v_d \gtrsim 100 \text{ km s}^{-1}$ through an ambient gas are known to be destroyed by nonthermal sputtering. Yet, previous studies of nonthermal sputtering disregarded the fact that dust grains can be spun-up to suprathreshold rotation by stochastic mechanical torques from gas-grain collisions. In this paper, we show that such grain suprathreshold rotation can disrupt a small grain into small fragments because induced centrifugal stress exceeds the maximum tensile strength of grain material, S_{max} . We term this mechanism *MEchanical Torque Disruption* (METD). We find that METD is more efficient than nonthermal sputtering in destroying smallest grains ($a < 10 \text{ nm}$) of nonideal structures moving with velocities of $v_d < 500 \text{ km s}^{-1}$. The ratio of rotational disruption to sputtering time is $\tau_{\text{disr}}/\tau_{\text{sp}} \sim 0.7(S_{\text{max}}/10^9 \text{ erg cm}^{-3})(\bar{A}_{\text{sp}}/12)(Y_{\text{sp}}/0.1)(a/0.01 \mu\text{m})^3(300 \text{ km s}^{-1}/v_d)^2$ where a is the radius of spherical grains, and Y_{sp} is sputtering yield. We also consider the high-energy regime and find that the rate of METD is reduced and becomes less efficient than sputtering for $v_d > 500 \text{ km s}^{-1}$ because impinging particles only transfer part of their momentum to the grain. We finally discuss implications of the METD mechanism for the destruction of hypersonic grains accelerated by radiation pressure as well as grains in fast shocks. Our results suggest that the destruction of small grains by METD in fast shocks of supernova remnants may be more efficient than previously predicted by nonthermal sputtering, depending on grain internal structures.

Keywords: dust, extinction, shock waves, supernova remnants

1. INTRODUCTION

The motion of dust grains at high velocities above $\sim 100 \text{ km s}^{-1}$ through the ambient gas (hereafter hypersonic motion) is common in the universe. Various physical processes can accelerate dust grains to hypersonic velocities, including radiation pressure induced by strong radiation sources (e.g., late-type stars, supernovae, and active galactic nuclei; Goldreich & Scoville 1976; Netzer & Elitzur 1993) and shock waves. Moreover, charged grains can be accelerated to high velocities in interstellar shocks of supernova remnants via betatron and Fermi acceleration mechanisms (Epstein 1980; Ellison et al. 1997). Magnetohydrodynamic turbulence is found to accelerate charged dust grains to high velocities (Yan et al. 2004; Hoang et al. 2012). In particular, newly formed dust grains in the supernova ejecta move hypersonically through the ambient gas before injected into the diffuse interstellar medium.

Hypersonic grain motion is thought to play an important role for a wide range of astrophysical phenomena such as galactic winds (e.g., Ishibashi & Fabian 2015), dust transport from the galaxy to the circumgalactic

and intergalactic medium (Ferrara et al. 1991; Aguirre et al. 2001a; Aguirre et al. 2001b; Bianchi & Ferrara 2005). Therefore, the critical question is whether dust grains can survive during the transport from the galaxy into the intergalactic medium (IGM). The survival of dust in the supernova ejecta is crucially important for quantifying the dust budget in the universe.

Nonthermal sputtering is believed to be a dominant mechanism for destruction of hypersonic grains (Draine & Salpeter 1979a). Thus, understanding the physics of sputtering is critically important for quantitative understanding of the formation and destruction of cosmic dust (see, e.g., Nozawa et al. 2006). The underlying physics of sputtering is that an impinging ion/atom can eject target atoms from the grain surface via nuclear-nuclear or electronic interactions (Sigmund 1981).

In fast shocks of velocities $v_{\text{sh}} \gtrsim 100 \text{ km s}^{-1}$, nonthermal sputtering is usually referred to explain the destruction of dust grains (Draine & Salpeter 1979a; Jones et al. 1994; Silvia et al. 2010). Observations reveal dust destruction in SNRs (Lakićević et al. 2015). Nevertheless, observations show that the fraction of dust destroyed

in fast shocks is higher than predicted by theoretical predictions based on sputtering (Williams et al. 2006; Sankrit et al. 2010; Zhu et al. 2019). This motivates us to look for physical effect ignored in the current theory of sputtering.

Indeed, previous studies of nonthermal sputtering disregarded the fact that the grain can be spun-up to suprathermal rotation by stochastic gas-grain collisions as pointed out by Gold (1952) and numerically demonstrated through Monte Carlo simulations by Purcell & Spitzer (1971). Recently, Hoang & Tram (2019) studied the effect of gas bombardment for nanoparticles drifting in steady-state shocks of low velocities of $v_{\text{sh}} < 50 \text{ km s}^{-1}$. The authors found that the smallest nanoparticles (size below 2 nm) can be spun-up to suprathermal rotation by stochastic mechanical torques and destroyed by centrifugal stress. This mechanism can be termed MEchanical Torque Disruption (METD). *The question is whether METD is still efficient for gas-grain collisions at higher velocities.*

The key difference between low and high-velocity gas-grain collisions is that, at high velocities (i.e., $v \gtrsim 50 \text{ km s}^{-1}$), incident particles may pass through instead of stick to the grain when the particle penetration length exceeds the grain diameter. As a result, they do not transfer their entire momentum to the grain upon collisions (Hoang 2017), and the efficiency of METD is reduced. The goal of this paper is to quantify the efficiency of METD for both low-energy (i.e., stick) and high-energy (passage) regimes and compare with nonthermal sputtering.

The structure of our paper is as follows. In Section 2, we study the spin-up and rotational disruption of grains by stochastic mechanical torques upon gas-grain collisions, and we compare METD with nonthermal sputtering in Section 3. Section 4 is devoted to discussing the implications of our study for dust destruction in fast shocks and grains accelerated by radiation pressure and its transport into the IGM. The summary of our main findings is presented in Section 5.

2. ROTATIONAL DISRUPTION BY STOCHASTIC TORQUES FROM GAS-GRAIN COLLISIONS

2.1. General consideration

We consider a spherical grain of radius a moving through the ambient gas of atomic hydrogen of temperature T_{gas} and number density n_{H} . Let define isothermal Mach sonic number $s_d = v_d/v_T$ where $v_T = (2kT_{\text{gas}}/m_{\text{H}})^{1/2} \simeq 1.2T_2^{1/2} \text{ km s}^{-1}$ with $T_2 = T_{\text{gas}}/(100 \text{ K})$ is the thermal gas velocity. For the supersonic regime of $s_d \gg 1$ considered in this paper, the

effect of thermal (Brownian) collisions is subdominant and can be ignored.

We first consider the *low-energy regime* where incident species collide and stick to the grain surface, such that they transfer their entire momentum to the grain. We then consider *high energy regime* where the penetration length of particles is larger than the grain diameter, such that they can pass through the grain, transferring part of their momentum to the grain (Hoang 2017).

2.2. Low-energy regime

2.2.1. Spin-up by stochastic torques from gas-grain collisions

Let us estimate the rotational excitation of grains due to sticking collisions of gas species. Each atom colliding with the grain surface at radius \mathbf{r} transfers its entire momentum $m_{\text{H}}v$ to the grain, inducing an *impulsive torque* of $\delta\mathbf{J} = \mathbf{r} \times m_{\text{H}}\mathbf{v}$ (see e.g., Gold 1952). The increase of $(\delta J)^2$ from each impact is given by

$$(\delta J)^2 = (a \cos \theta m_{\text{H}} v_d)^2 = m_{\text{H}}^2 v_d^2 a^2 \cos^2 \theta, \quad (1)$$

where θ is the polar angle of the radius vector \mathbf{r} , and the projectiles are impinging along the horizontal plane.

By averaging the above equation over the grain surface, one has $\langle \cos^2 \theta \rangle = 1/2$. Thus, Equation (1) becomes

$$\langle (\delta J)^2 \rangle = \frac{1}{2} m_{\text{H}}^2 v_d^2 a^2, \quad (2)$$

which yields the rotational angular velocity acquired by a single collision:

$$\delta\omega = \frac{\langle (\delta J)^2 \rangle^{1/2}}{I} \simeq 1.6 \times 10^7 a_{-6}^{-4} v_3 \text{ rad s}^{-1}, \quad (3)$$

where the inertia moment $I = 8\pi\rho a^5/15$ with ρ the grain mass density, $a_{-6} = a/(10^{-6} \text{ cm})$, and $v_3 = v_d/(10^3 \text{ km s}^{-1})$.

Using the random walk theory for stochastic collisions, one can derive the total increase of squared angular momentum per unit of time as follows:

$$\frac{\langle (\Delta J)^2 \rangle}{\Delta t} = R_{\text{coll}} (\delta J)^2 = \frac{n_{\text{H}} v_d \pi a^2 m_{\text{H}}^2 v_d^2 a^2}{2}, \quad (4)$$

where the collision rate $R_{\text{coll}} = n_{\text{H}} v_d \pi a^2$ has been used.

After traversing a time interval Δt , the total average increase of the squared angular momentum is equal to

$$\langle (\Delta J)^2 \rangle = \frac{n_{\text{H}} m_{\text{H}}^2 v_d^3 \pi a^4}{2} \Delta t. \quad (5)$$

The *rms* angular velocity of grains can now be calculated using the total angular momentum ΔJ from Equation (5):

$$\omega_{\text{rms}}^2 = \langle \omega^2 \rangle = \frac{\langle (\Delta J)^2 \rangle}{I^2} = \frac{n_{\text{H}} m_{\text{H}}^2 v_d^3 \pi a^4}{2I^2} \Delta t. \quad (6)$$

A rotating grain experiences rotational damping due to sticking collision with gas atoms. Note that sticking collisions do not damp grain rotation due to averaging effect, but subsequent thermal evaporation of atoms that carry away part of the grain angular momentum results in grain rotational damping (see e.g., [Draine & Lazarian 1998](#)). Consider a grain rotating along the z -axis with angular velocity ω_z . The angular momentum carried away by an H atom from the grain surface is given by

$$\delta J_z = I_m \omega_z = m_H r^2 \omega_z = m_H a^2 \sin^2 \theta \omega_z, \quad (7)$$

where r is the distance from the atom to the spinning axis z , $I_m = m_H r^2$ is the inertial moment of the hydrogen atom of mass m_H , θ is the angle between the z -axis and the radius vector, and $r = a \sin \theta$ is the projected distance to the center. Assuming the isotropic distribution of θ for atoms leaving the grain, one can replace $\sin^2 \theta = \langle \sin^2 \theta \rangle = 2/3$, which give rise to

$$\langle \delta J_z \rangle = \frac{2}{3} m_H a^2 \omega_z. \quad (8)$$

Using the collision rate of atomic gas, R_{coll} , one can derive the mean decrease of grain angular momentum per unit of time is

$$\left\langle \frac{\Delta J_z}{\Delta t} \right\rangle_{\text{H}} = -R_{\text{coll}} \langle \delta J_z \rangle = -\frac{2}{3} n_H m_H \pi a^4 \omega_z \langle v \rangle = -\frac{I \omega_z}{\tau_H}. \quad (9)$$

For the drift velocity with $v \gg v_T$, one has $\langle v \rangle = v_d$. Therefore, the rotational damping time is

$$\tau_H = \frac{3I}{2n_H m_H \pi a^4 v_d} = \frac{4\rho a}{5n_H m_H v_d} \simeq 572 \left(\frac{\hat{\rho}_{a-6}}{v_2 n_1} \right) \text{ yr}, \quad (10)$$

where $n_1 = n/(10 \text{ cm}^{-3})$, $\hat{\rho} = \rho/(3 \text{ g cm}^{-3})$, $v_2 = v_d/(100 \text{ km s}^{-1})$.

Rapidly spinning dust grains emit strong electric dipole radiation ([Draine & Lazarian 1998](#)), which also damps the grain rotation on a timescale of

$$\tau_{\text{ed}} = \frac{3I^2 c^3}{\mu^2 k T_{\text{gas}}} \simeq 2.25 \times 10^8 \left(\frac{a_{-6}^7}{3.8 \hat{\beta}} \right) \left(\frac{100 \text{ K}}{T_{\text{gas}}} \right) \text{ yr} \quad (11)$$

where μ is the grain dipole moment and $\hat{\beta} = \beta/(0.4D)$ with β being the dipole moment per structure due to polar bonds present in the dust grain ([Draine & Lazarian 1998](#); [Hoang et al. 2010](#); [Hoang et al. 2016](#)).

Comparing τ_{ed} with τ_H , one can see that, for small grains of $a > 1 \text{ nm}$, the electric dipole damping time is longer than the gas damping time.

Due to the rotational damping, the grain loses angular momentum on a timescale of τ_H . Therefore, Equation (6) yields

$$\omega_{\text{rms}}^2 \equiv \langle \omega^2 \rangle = \frac{n_H m_H^2 v^3 \pi a^4}{2I^2} \tau_H, \quad (12)$$

which can be rewritten as

$$\frac{\omega_{\text{rms}}^2}{\omega_T^2} = \frac{s_d^2}{2}, \quad (13)$$

where the thermal angular velocity

$$\omega_T = \left(\frac{3kT_{\text{gas}}}{I} \right)^{1/2} \simeq 9 \times 10^7 a_{-6}^{-5/2} T_2^{1/2} \hat{\rho}^{-1/2} \text{ rad s}^{-1}. \quad (14)$$

2.2.2. Mechanical Torque Disruption Mechanism

The basic idea of rotational disruption by stochastic mechanical torques (i.e., METD mechanism), is as follows. A spherical dust grain rotating at velocity ω develops a centrifugal stress due to centrifugal force, which is maximum along the plane through the grain center of $S = \rho a^2 \omega^2 / 4$ ([Hoang et al. 2019](#)). When the rotation rate increases to a critical limit such that the tensile stress induced by centrifugal force exceeds the maximum tensile stress, the so-called tensile strength of the material, the grain is disrupted instantaneously. The critical angular velocity for the disruption is given by

$$\omega_{\text{cri}} = \frac{2}{a} \left(\frac{S_{\text{max}}}{\rho} \right)^{1/2} \simeq 3.65 \times 10^{10} \left(\frac{S_{\text{max},9}^{1/2}}{a_{-6} \hat{\rho}^{1/2}} \right) \text{ rad s}^{-1}, \quad (15)$$

where S_{max} is the tensile strength of dust material and $S_{\text{max},9} = S_{\text{max}}/(10^9 \text{ erg cm}^{-3})$ is the tensile strength in units of 10^9 erg cm^{-3} . An alternative unit of the tensile strength is dyne/cm^2 , but in this paper we use the unit of erg cm^{-3} for S_{max} .

The tangential velocity required for the disruption is

$$v_{\text{cri}} \sim \omega_{\text{cri}} a \sim 0.36 \left(\frac{S_{\text{max},9}^{1/2}}{\hat{\rho}^{1/2}} \right) \text{ km s}^{-1}, \quad (16)$$

which is much smaller than the gas thermal velocity of $v_T \sim 1.2 T_2^{1/2} \text{ km s}^{-1}$.

The exact value of S_{max} depends on grain composition and structure. Compact grains are expected to have higher S_{max} than porous/composite grains. Ideal material without impurity, such as diamond, can have $S_{\text{max}} \geq 10^{11} \text{ erg cm}^{-3}$ (see [Hoang et al. 2019](#) for more details). In the following, grains with $S_{\text{max}} \gtrsim 10^9 \text{ erg cm}^{-3}$ are referred to as strong materials, and those with $S_{\text{max}} < 10^9 \text{ erg cm}^{-3}$ are called weak materials.

2.2.3. Disruption time and disruption size

The time required to spin-up a grain of size a to ω_{cri} , so-called rotational disruption time, is evaluated as follows:

$$\begin{aligned} \tau_{\text{disr}} &= \frac{J_{\text{cri}}^2}{(\Delta J)^2/(\Delta t)} = \frac{2(I\omega_{\text{cri}})^2}{n_{\text{H}}m_{\text{H}}^2v_d^3\pi a^4} = \frac{512\pi a^4\rho S_{\text{max}}}{225n_{\text{H}}m_{\text{H}}^2v_d^3} \\ &\simeq 2.4 \times 10^4 \left(\frac{a_{-6}^4}{v_2^3}\right) \left(\frac{S_{\text{max},9}}{n_1\hat{\rho}}\right) \text{yr} . \end{aligned} \quad (17)$$

The above equation implies that nanoparticles of $a \sim 1$ nm moving at $v_d \sim 100$ km s⁻¹ are disrupted in $t_{\text{disr}} \sim 2$ yr, while the grain rotation is damped in $\tau_{\text{H}} \sim 50$ yr by gas collisions or in $\tau_{\text{ed}} \sim 20$ yr by electric dipole emission.

We note that METD only occurs when the required time is shorter than the rotational damping time. Let a_{disr} be the grain disruption size as determined by $\tau_{\text{disr}} = \tau_{\text{H}}$. Thus, comparing Equations (17) and (10), one obtains:

$$a_{\text{disr}} = \left(\frac{25m_{\text{H}}v_d^2}{128\pi S_{\text{max}}}\right)^{1/3} \simeq 5.5S_{\text{max},9}^{-1/3} \left(\frac{v_d}{300\text{km s}^{-1}}\right)^{2/3} \text{nm} \quad (18)$$

which implies that very small grains ($a < 5$ nm) moving at $v_d \sim 300$ km s⁻¹ are disrupted by centrifugal stress, assuming strong grains of $S_{\text{max}} \sim 10^9$ erg cm⁻³. The rotation of larger grains (i.e., $a > a_{\text{disr}}$) is damped by gas collisions before reaching the critical threshold.

For a given grain size, the critical speed required for rotational disruption is given by the condition of $\tau_{\text{disr}} \lesssim \tau_{\text{H}}$, which yields

$$v_d \gtrsim \left(\frac{128\pi a^3 S_{\text{max}}}{45m_{\text{H}}}\right)^{1/2} \simeq 733a_{-6}^{3/2} S_{\text{max},9}^{1/2} \text{km s}^{-1}. \quad (19)$$

or the dimensionless parameter:

$$s_d \gtrsim \left(\frac{64\pi a^3 S_{\text{max}}}{45kT_{\text{gas}}}\right)^{1/2} \simeq 565a_{-6}^{3/2} T_2^{-1/2} S_{\text{max},9}^{1/2}. \quad (20)$$

The above equations indicate that the velocity required for METD decreases rapidly with decreasing grain size and with tensile strength. Smallest nanoparticles of sizes $a \sim 1$ nm only require $v_d \sim 23$ km s⁻¹ while small grains of $a \sim 0.01$ μm require much higher velocities for rotational disruption, assuming $S_{\text{max}} \lesssim 10^9$ erg cm⁻³.

The rotation of nanoparticles experiences damping and excitation by various interaction processes, including ion collisions, plasma drag, and infrared emission (see [Draine & Lazarian 1998](#); [Hoang et al. 2010](#)). A detailed analysis of the different damping processes for grains in magnetized shocks is presented in [Hoang & Tram \(2019\)](#) and [Tram & Hoang \(2019\)](#).

2.2.4. Slowing-down time by gas drag force

For hypersonic grains, the main gas drag arises from direct collisions with gas atoms, and the Coulomb drag force is subdominant ([Draine & Salpeter 1979b](#)). Assuming the sticky collisions of atoms followed by their thermal evaporation, the decrease in the grain momentum is equal to the momentum transferred to the grain in the opposite direction:

$$F_{\text{drag}} \equiv \frac{dP}{dt} = m_{\text{H}}v_d \times n_{\text{H}}v_d\pi a^2. \quad (21)$$

The gas drag time is given by

$$\begin{aligned} \tau_{\text{drag}} &= \frac{m_{\text{gr}}v_d}{dP/dt} = \frac{4\pi\rho a^3v_d}{3\pi a^2n_{\text{H}}v_d^2m_{\text{H}}} \\ &= \frac{4\rho a}{3n_{\text{H}}m_{\text{H}}v_d} \simeq 763 \left(\frac{\hat{\rho}a_{-6}}{n_1v_2}\right) \text{yr}. \end{aligned} \quad (22)$$

Comparing Equations (22) with (17) one can see that the disruption occurs much faster than the drag time for $v > 100$ km s⁻¹ and small grains of $a < 0.01$ μm .

2.3. High-energy regime

The penetration depth of impinging protons is approximately equal to ([Draine & Salpeter 1979b](#)):

$$R_{\text{H}}(E) \simeq \left(\frac{0.01}{\hat{\rho}}\right) \left(\frac{E}{1 \text{ keV}}\right) \mu\text{m} \simeq 0.008 \left(\frac{v_2^2}{\hat{\rho}}\right) \mu\text{m} \quad (23)$$

which reveals that for high-velocity collisions, impinging particles can pass through the grain because $R_{\text{H}} > 2a$. As a result, they only transfer part of their momentum to the grain. We will first find the fraction of ion momentum transferred to the grain and quantify the efficiency of METD.

For interstellar grains with $a < 1$ μm and energetic ions, we have $\Delta E \ll p^2/2m$, [Hoang \(2017\)](#) derived

$$\delta p = \frac{2mp\delta E}{2p^2 - m\delta E} \approx p \left(\frac{\delta E}{2E}\right) = pf_p(E, a), \quad (24)$$

where ΔE is the energy loss passing the grain, and $f_p(E, a) = \delta E/(2E)$ is the fraction of the ion energy transferred to the grain which is a function of E and a .

Let $dE/dx = nS(E)$ where $S(E)$ be the stopping cross-section of the impinging ion of kinetic energy E in the dust grain of atomic density n ([Sigmund 1981](#)). The energy loss of the ion due to the passage of the grain is given by

$$\delta E = \frac{4a}{3}nS(E), \quad (25)$$

where the grain is approximated as slab of thickness $4a/3$. Thus,

$$f_p = \frac{2a}{3E}nS(E), \quad (26)$$

and $f_p(E, a) = 1$ for sticking collisions.

Following Equation (2), the impulsive angular momentum from a collision is then given by

$$(\delta J)^2 = \frac{a^2}{2}(\delta p)^2 = \frac{a^2 p^2}{2} f_p(E, a)^2. \quad (27)$$

which yields the average value

$$\langle (\delta J)^2 \rangle = \frac{a^2 p^2}{2} f_p(E, a)^2. \quad (28)$$

Following the similar procedure as in Section 2, one obtain

$$\left\langle \frac{(\Delta J)^2}{\Delta t} \right\rangle = \left\langle \frac{(\Delta J)^2}{\Delta t} \right\rangle_S f_p^2, \quad (29)$$

where S denotes sticking collisions considered in the previous subsection, and $\langle \frac{(\Delta J)^2}{\Delta t} \rangle_S$ is given by Equation (4).

The increase of the grain angular velocity is given by

$$\omega_{\text{rms}}^2 = \frac{(\Delta J)^2 / \Delta t}{I^2} \times t = \left(\frac{n_{\text{H}} m_{\text{H}} v^3 \pi a^4}{2I^2} \right) f_p^2 \times t. \quad (30)$$

If the incident ion passes through the grain, the grain rotational damping by gas collisions is not important, and the damping by electric dipole emission takes over. Since τ_{ed} is rather long for nanoparticles of $a > 1$ nm (see Hoang et al. 2010), the grain angular velocity continues to increase to the critical limit, i.e., at ω_{disr} , i.e., the disruption occurs, in disruption time equal to

$$\tau_{\text{disr}} = \left(\frac{2I\omega_{\text{disr}}^2}{n_{\text{H}} m_{\text{H}} v^3 \pi a^4} \right) \frac{1}{f_p^2} = \tau_{\text{disr},S} \left(\frac{1}{f_p^2} \right), \quad (31)$$

where $\tau_{\text{disr},S}$ is the disruption time for sticky collisions given by Equation (17). The rate of rotational disruption is decreased rapidly with E when $f_p < 1$. In the above analysis, we assumed a slab model to calculate the fraction of the momentum transfer. As shown in Appendix A, this assumption induces a negligible difference to the more detailed treatment.

For grain velocity below the Bohr velocity of $v_0 = e^2/\hbar \approx c/137 \approx 2189$ km s⁻¹, nuclear interactions dominate, and the stopping cross-section in units of erg cm² is given by (Sigmund 1981)

$$S_n(E) = 4.2\pi a Z_1 Z_2 e^2 \frac{M_1}{(M_1 + M_2)} s_n(\epsilon_{12}), \quad (32)$$

where M_i and Z_i are the atomic masses and numbers charge of the projectile ($i = 1$) and target ($i = 2$) atom, and a is the screen length for the nuclei-nuclei interaction potential given by

$$a \simeq 0.885 a_0 (Z_1^{2/3} + Z_2^{2/3})^{-1/2}, \quad a_0 = 0.529 \text{ \AA}, \quad (33)$$

and

$$\epsilon_{12} = \left(\frac{M_2 E}{M_1 + M_2} \right) \left(\frac{a}{Z_1 Z_2 e^2} \right). \quad (34)$$

We adopt the approximate function of s_n as in Tielens et al. (1994):

$$s_n = \frac{3.441 \sqrt{\epsilon_{12}} \ln(\epsilon_{12} + 2.718)}{1 + 6.35 \sqrt{\epsilon_{12}} + \epsilon_{12}(-1.708 + 6.882 \sqrt{\epsilon_{12}})}. \quad (35)$$

For grain velocities above v_0 , electronic interactions dominate, and the stopping power can be approximated as

$$nS_e(E) \approx \frac{2nS_m(E/E_m)^\eta}{1 + (E/E_m)}, \quad (36)$$

where η is the slope, $E_m = 100$ keV and S_m is the stopping power at $E = E_m$. For graphite, we find that $\eta = 0.2$ and $nS_m = 1.8 \times 10^6$ keV/cm. For quartz material, $\eta = 0.25$ and $nS_m = 1.3 \times 10^6$ keV/cm.

Drag force in the high-velocity regime is given by (see also Hoang 2017)

$$F_{\text{drag}} = R_{\text{coll}} \delta p = n_{\text{H}} \pi a^2 m_{\text{H}} v_d^2 \left(\frac{1}{2f_p} \right). \quad (37)$$

The drag time is equal to

$$\tau_{\text{drag}} = \frac{m_{\text{gr}} v_d}{F_{\text{drag}}} = \tau_{\text{drag},S} \left(\frac{1}{2f_p} \right), \quad (38)$$

where $\tau_{\text{drag},S}$ is given by Equation (22).

2.4. Nonthermal sputtering

To prepare for comparison, we discuss here nonthermal sputtering which is previously thought to be an efficient mechanism to destroy small grains upon gas-grain collisions (e.g., Draine & Salpeter 1979a; Jones et al. 1994).

Let Y_{sp} be the average sputtering yield per impinging atom (i.e., H and He) with velocity v_d . Let dN_{sp} be the number of target atoms sputtered by the bombardment per second, which is given by

$$\frac{dN_{\text{sp}}}{dt} = n_{\text{H}} v_d \pi a^2 Y_{\text{sp}}. \quad (39)$$

The rate of grain mass loss due to nonthermal sputtering is given by (see e.g., Hoang et al. 2015)

$$\frac{4\pi \rho a^2 da}{dt} = m_{\text{sp}} \frac{dN_{\text{sp}}}{dt} = \bar{A}_{\text{sp}} m_{\text{H}} n_{\text{H}} v_d \pi a^2 Y_{\text{sp}}, \quad (40)$$

which yields

$$\begin{aligned} \frac{da}{dt} &= \frac{n_{\text{H}} m_{\text{H}} v_d Y_{\text{sp}} \bar{A}_{\text{sp}}}{4\rho}, \\ &\simeq 5.2 \times 10^{-6} \left(\frac{\bar{A}_{\text{sp}}}{12} \right) \left(\frac{n_1 v_2}{\hat{\rho}} \right) \left(\frac{Y_{\text{sp}}}{0.1} \right) \frac{\mu\text{m}}{\text{yr}}, \end{aligned} \quad (41)$$

where $m_{\text{sp}} = \bar{A}_{\text{sp}} m_{\text{H}}$ with \bar{A}_{sp} the average atomic mass number of sputtered atoms. Above, we consider the projectiles along the normal vector only.

The sputtering yield, Y_{sp} , depends on projectile energy and properties of grain material. Following Tielens et al. (1994), the sputtering yield is given by

$$Y_{\text{sp}}(E) = 4.2 \times 10^{14} \frac{\alpha S_n(E)}{U_0} \left(\frac{R_p}{R} \right) \times \left[1 - (E_{\text{th}}/E)^{2/3} \right] (1 - E_{\text{th}}/E)^2, \quad (42)$$

where U_0 is the binding energy of dust atoms, $\alpha \simeq 0.3(M_2/M_1)^{2/3}$ for $0.5 < M_2/M_1 < 10$, $\alpha \approx 0.1$ for $M_2/M_1 < 0.5$, and E_{th} is the threshold energy for sputtering given by

$$E_{\text{th}} = \frac{U_0}{g(1-g)} \text{ for } M_1/M_2 \leq 0.3, \quad (43)$$

$$E_{\text{th}} = 8U_0 \left(\frac{M_1}{M_2} \right)^{1/3} \text{ for } M_1/M_2 > 0.3, \quad (44)$$

and $g = 4M_1M_2/(M_1 + M_2)^2$ is the maximum energy transfer of a head-on elastic collision. The factor R_p/R is the ratio of the mean projected range to the mean penetrated path length, as given by (Bohdansky 1984)

$$\frac{R_p}{R} = \left(K \frac{M_2}{M_1} + 1 \right)^{-1} \quad (45)$$

where K is a free parameter, and $K = 0.1$ and 0.65 for silicate and graphite grains, respectively (see Tielens et al. 1994).

The characteristic timescale of grain destruction by nonthermal sputtering for a grain of size a is defined by

$$\tau_{\text{sp}} = \frac{a}{da/dt} = \frac{4\rho a}{n_{\text{H}} m_{\text{H}} v_d Y_{\text{sp}} \bar{A}_{\text{sp}}} \simeq 1.9 \times 10^3 \hat{\rho} \left(\frac{12}{\bar{A}_{\text{sp}}} \right) \left(\frac{a_{-6}}{n_1 v_2} \right) \left(\frac{0.1}{Y_{\text{sp}}} \right) \text{yr}. \quad (46)$$

3. NUMERICAL RESULTS

For numerical results shown in this section, we assume graphite grains ($\rho = 2.2 \text{ g cm}^{-3}$, $U_0 = 4 \text{ eV}$) moving through purely hydrogen gas with gas density $n_{\text{H}} = 10 \text{ cm}^{-3}$ and $T_{\text{gas}} = 100 \text{ K}$. The present theory can be applied to arbitrary grain materials and astrophysical environments.

3.1. Grain disruption time

To obtain the disruption time by METD, we first calculate the fraction of particle momentum transferred to the grain upon collisions for the different velocity using Equation (26). The obtained results are shown in

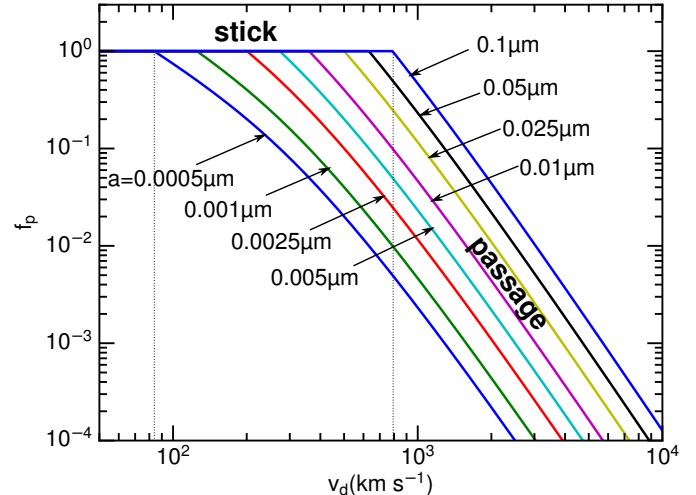


Figure 1. The fraction of proton momentum transferred to the grain, f_p , as a function of grain velocity for the different grain sizes a from $0.0005 \mu\text{m}$ to $0.1 \mu\text{m}$. Graphite material is considered. Stick regime $f_p = 1$ and passage regime ($f_p < 1$) are separated by a vertical dotted line.

Figure 1. For low velocities ($v_d < 100 \text{ km s}^{-1}$), $f_p = 1$, which correspond to the sticking that impinging particles collide and stick to the grain. For high velocities, f_p decreases rapidly with increasing v_d due to the passage of incident particles. The transition velocity from the stick to passage regimes increases with grain size.

We calculate the characteristic timescale of METD using Equations (17) and (31) for the different grain sizes. The drift velocity v_d is varied to cover both the low-energy regime (stick) and high-energy (passage) regime. The tensile strength is also varied to reflect different grain structures. We also calculate the timescales of rotational damping by gas collisions and electric dipole emission, gas drag, and sputtering using Equations (10), (11), (22), and (46) and compare the obtained results with the METD time.

Figure 2 shows the METD timescale compared to the various timescales, assuming the different grain sizes and tensile strength. The shaded regions mark the parameter space where METD is faster than nonthermal sputtering, characterized by $\tau_{\text{disr}} \leq \tau_{\text{sp}}$. The METD time rapidly decreases with grain velocity v_d during the low-energy regime where impinging particles stick to the grain and transfer their entire momentum to the grain ($f_p = 1$). When v_d becomes sufficiently large, impinging particles just pass through the grain, and τ_{disr} reverses the trend and increases with increasing v_d due to the reduction of the ion momentum transfer to the grain (i.e., $f_p < 1$).

For small grains of $a = 0.001 \mu\text{m}$, METD is faster than sputtering for velocities of $v_d < 180 \text{ km s}^{-1}$ for ideal

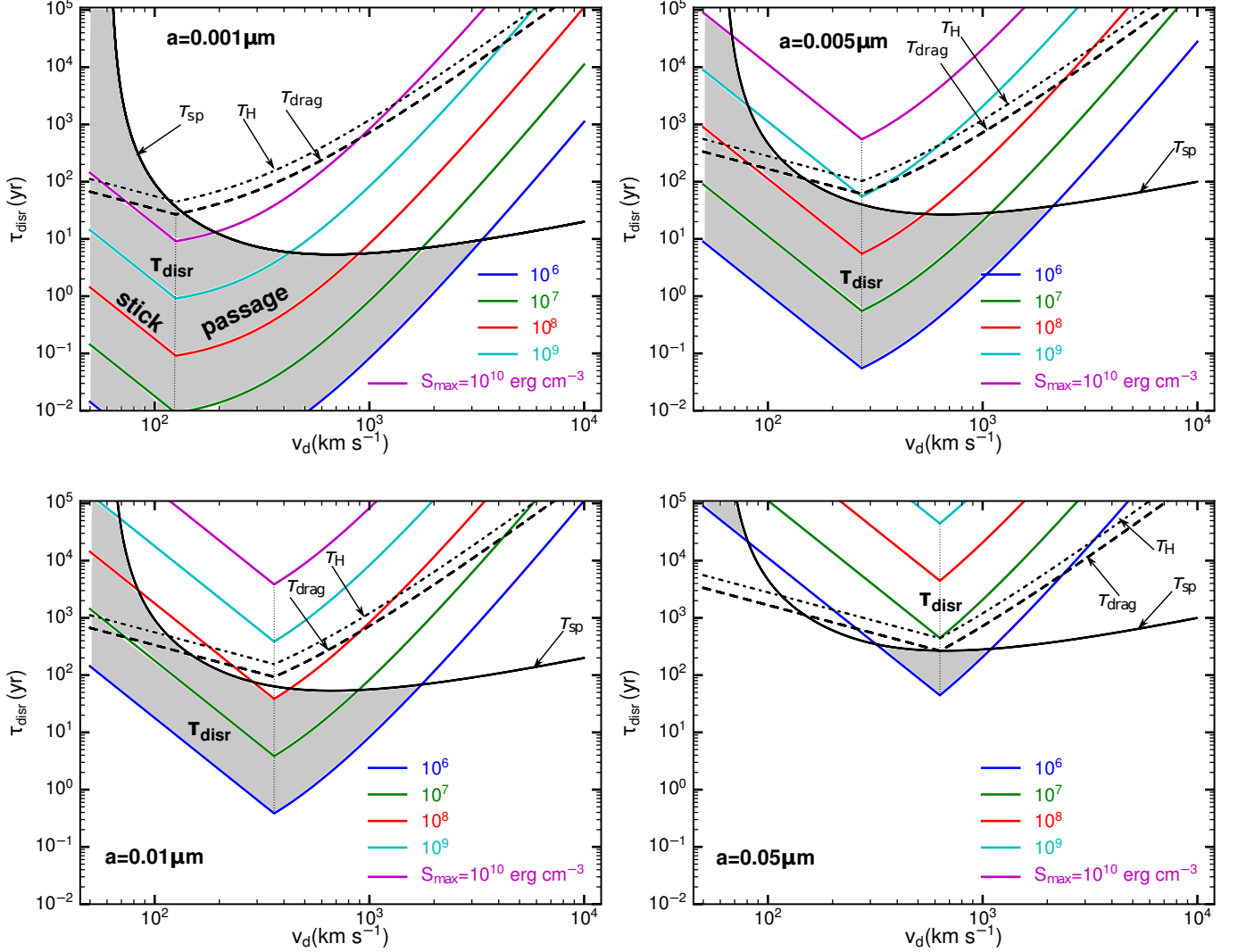


Figure 2. The METD timescale vs. the grain velocity for the different grain sizes and tensile strength S_{\max} . The timescales of nonthermal sputtering, gas drag, rotational damping, and electric dipole damping are overplotted for comparison. Shaded regions correspond to $\tau_{\text{disr}} \leq \tau_{\text{sp}}$. The vertical line mark the transition from stick to passage regimes.

material of $S_{\max} = 10^{10} \text{ erg cm}^{-3}$. For weak materials of $S_{\max} \sim 10^7 \text{ erg cm}^{-3}$ (e.g., fluffy grains), METD is much faster than sputtering for $v_d < 1500 \text{ km s}^{-1}$. For large grains of $a = 0.05 \mu\text{m}$, rotational disruption is only effective for grains with low tensile strength of $S_{\max} \sim 10^6 \text{ erg cm}^{-3}$ at $v_d \sim 300 - 1000 \text{ km s}^{-1}$.

Figures 3 shows the METD timescale as a function of the grain size for different tensile strength and $v_d = 50 - 300 \text{ km s}^{-1}$. METD is faster than gas drag as well as sputtering for small grains and high velocities. At low velocities $v_d \leq 100 \text{ km s}^{-1}$, impinging particles collide and stick to the grain surface, and τ_{disr} decreases rapidly with grain size (upper panels). At higher velocities, incident particles can pass through the grain if

their sizes are small (see lower panels), resulting in the change in the slope of τ_{disr} vs. a .

Figure 4 shows the similar result for higher velocities of $v_d = 400 - 1000 \text{ km s}^{-1}$. The range of grain sizes where METD is efficient is narrower for higher v_d . This arises from the decrease of ion momentum transfer to the grain at very high v_d (see Figure 1).

From Equations (17) and (46) one obtains the ratio of METD time to nonthermal sputtering time:

$$\frac{\tau_{\text{disr}}}{\tau_{\text{sp}}} \simeq 6.4 S_{\max,9} \left(\frac{\bar{A}_{\text{sp}}}{12} \right) \left(\frac{Y_{\text{sp}}}{0.1} \right) \left(\frac{a^3}{v_d^2} \right) f_p^{-2}, \quad (47)$$

where $f_p = 1$ for low velocities but decreases rapidly with increasing v_d at very high velocities (see Eq. 26).

Equation (47) reveals that the METD mechanism is faster than nonthermal sputtering for small grains (e.g.,

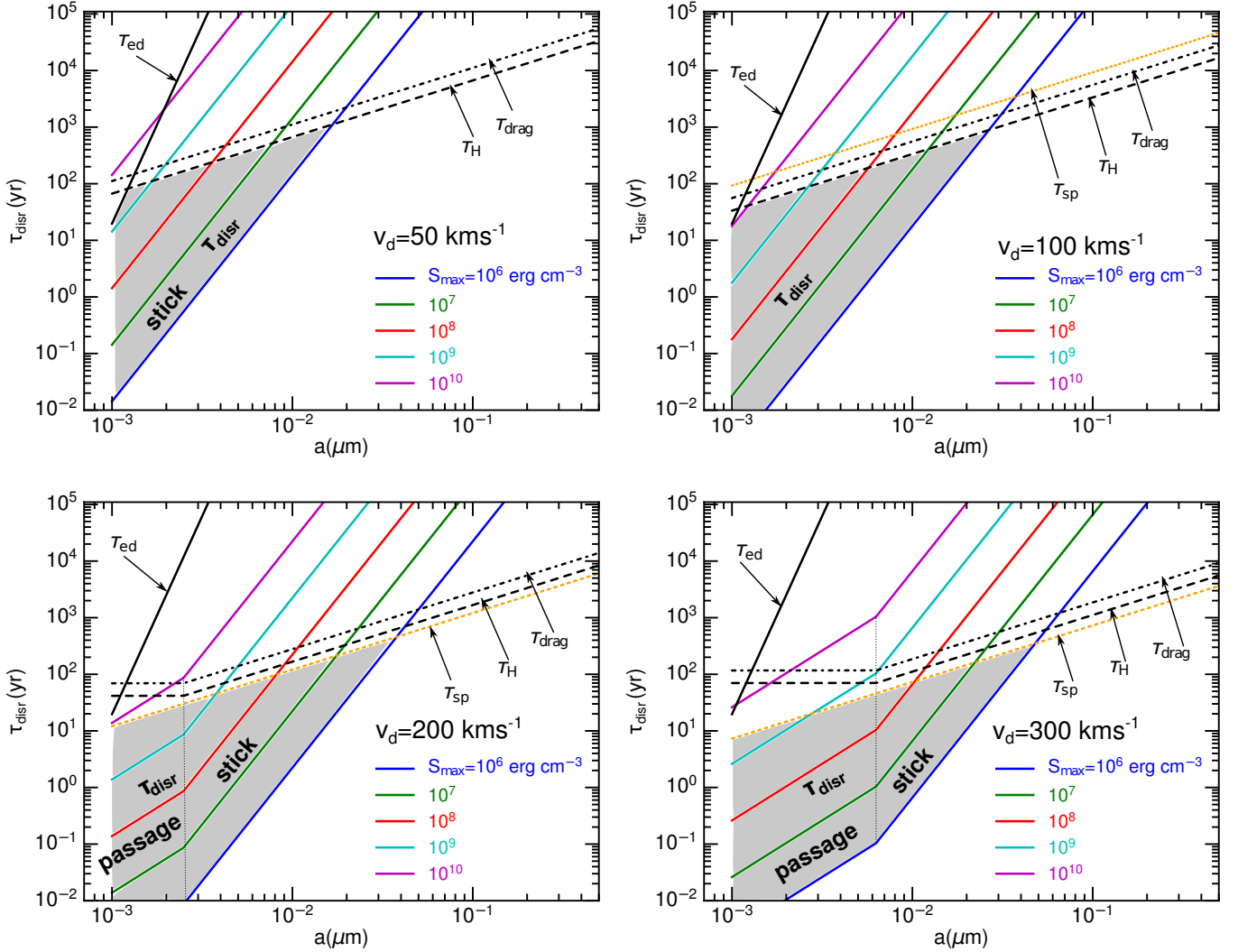


Figure 3. Characteristic timescale of METD vs. grain size for the different grain velocities and tensile strength. Timescales of gas drag, rotational damping by gas collisions and electric dipole emission, and nonthermal sputtering are shown for comparison. Shaded areas represent the space where METD is faster than other processes. The vertical line mark the transition from the passage to stick regimes.

nanoparticles). Indeed, from Equation (3) one can see that a single collision can spin up the grain to $\delta\omega \sim 10^7 a_{-6}^{-4} v_3 \text{ rad s}^{-1}$. Thus, to spin-up the $0.01 \mu\text{m}$ grain to the disruption limit, $\omega_{\text{cri}} \sim 10^9 \text{ rad s}^{-1} S_{\text{max},9}^{1/2}$, it only requires $N_{\text{disr}} \sim (\omega_{\text{cri}}/\delta\omega)^2 \sim 10^4$ random collisions. However, nonthermal sputtering of yield $Y_{\text{sp}} \sim 0.1$ requires $N_{\text{at}}/Y_{\text{sp}} \sim 10^6$ collisions to completely destroy the grain where N_{at} is the total number of atoms in the dust grain.

3.2. Grain disruption sizes

To obtain grain disruption size a_{disr} for arbitrary velocities v_d , we first calculate τ_{disr} for a range of grain sizes and compare with rotational damping time τ_H . As shown in Figures 3 and 4, METD becomes faster than

nonthermal sputtering for grains smaller than the value at the intersection (i.e., $\tau_{\text{disr}} = \tau_{\text{sp}}$), which is denoted by $a_{\text{disr,sp}}$.

Figure 5 (left panel) shows the values of a_{disr} as a function of grain velocity for various tensile strength. The disruption size a_{disr} increases with increasing v_d and then decreases due to the decrease of ion momentum transfer to the grain ($f_p < 1$).

Figure 5 (right panel) shows the variation of $a_{\text{disr,sp}}$ with v_d . Shaded areas mark the parameter space (v_d, a) in which METD is faster than nonthermal sputtering. For weak grains (e.g., of fluffy structure) with $S_{\text{max}} \sim 10^7 \text{ erg cm}^{-3}$, grains of $a \sim 0.02 \mu\text{m}$ can be disrupted for $v_d < 600 \text{ km s}^{-1}$. For very strong grains of ideal structures with $S_{\text{max}} \sim 10^9 \text{ erg cm}^{-3}$, very small

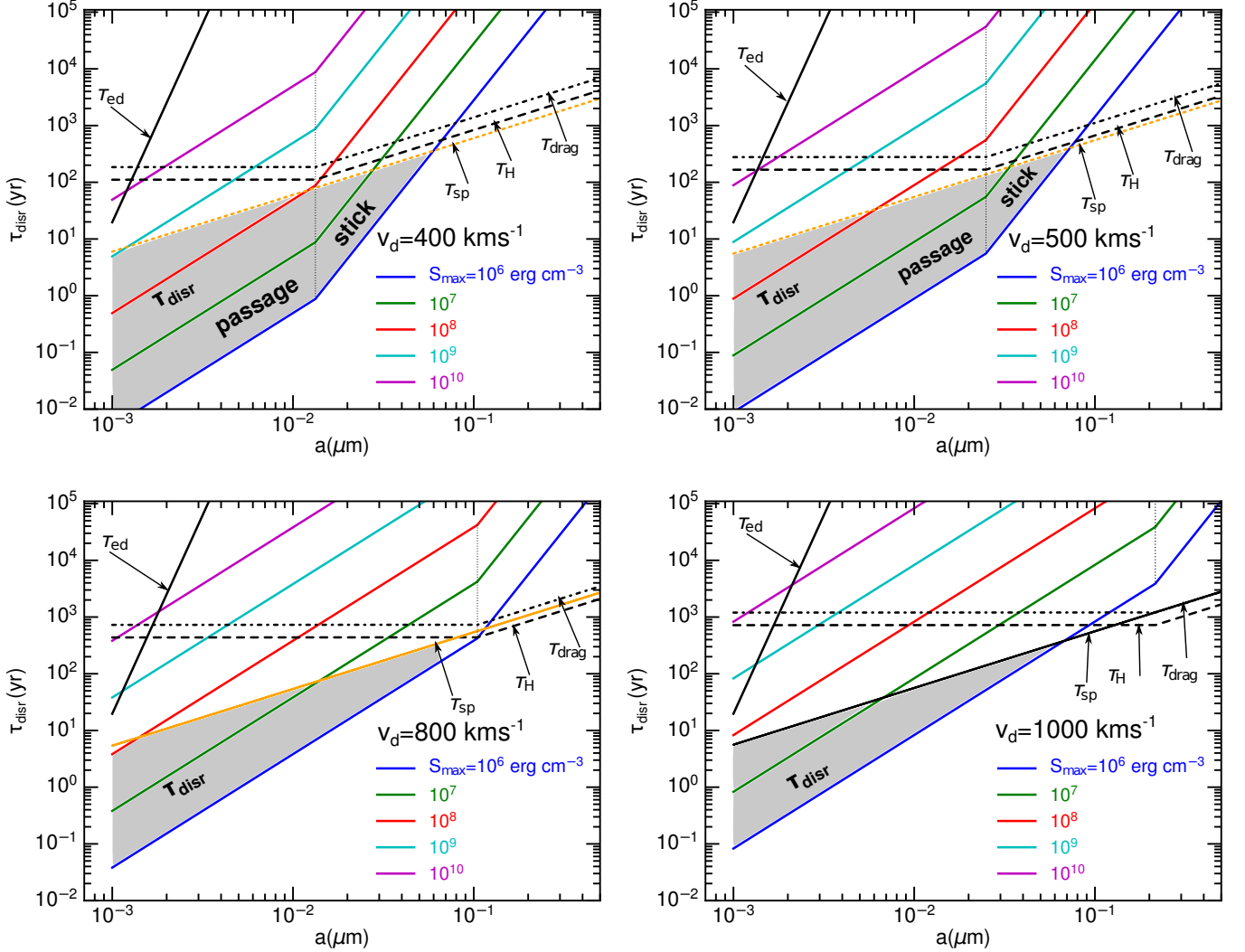


Figure 4. Same as Figure 2 but for velocities $v_d \geq 400 \text{ km s}^{-1}$. METD becomes less efficient due to the degree of ion momentum transfer to the grain but still important for small grains of non-ideal structures.

grains of $a \sim 0.004 \mu\text{m}$ can be rotational disrupted for $v_d < 250 \text{ km s}^{-1}$. Nonthermal sputtering dominates the destruction of large grains (i.e., $a > 0.1 \mu\text{m}$) or at high velocities of $v_d > 1000 \text{ km s}^{-1}$.

4. DISCUSSION

4.1. The importance of grain internal structures for dust destruction by gas-grain collisions

Internal structures (compact vs. porous) of dust grains are essential for dust absorption and emission (Guillet et al. 2017). The grain internal structure determines the mechanical strength of grains as measured by tensile strength. Indeed, grain internal structures are found to play an important role for grain coagulation (Dominik & Tielens 1997). However, this property is previously ignored in the destruction process by gas-grain collisions (thermal and nonthermal processes).

Very recently, with the discovery of RAdiative Torque Disruption (RATD) mechanism (Hoang et al. 2019), the grain tensile strength is crucially important in determining the upper cutoff of the grain size distribution (Hoang 2019). Our present study reveals that the tensile strength also plays a critical role in dust destruction by gas-grain collisions. Small grains ($a < 0.01 \mu\text{m}$) of fluffy structures with low tensile strength ($S_{\text{max}} < 10^9 \text{ erg cm}^{-3}$) can be destroyed more efficiently than nonthermal sputtering when moving at high velocities through the gas. While nonthermal sputtering does depend on the internal structure of grains (e.g., only on the binding energy of target atoms), rotational disruption critically depends on the tensile strength S_{max} . Very small grains ($a \lesssim 1 \text{ nm}$) can be destroyed by METD even when they have ideal structures.

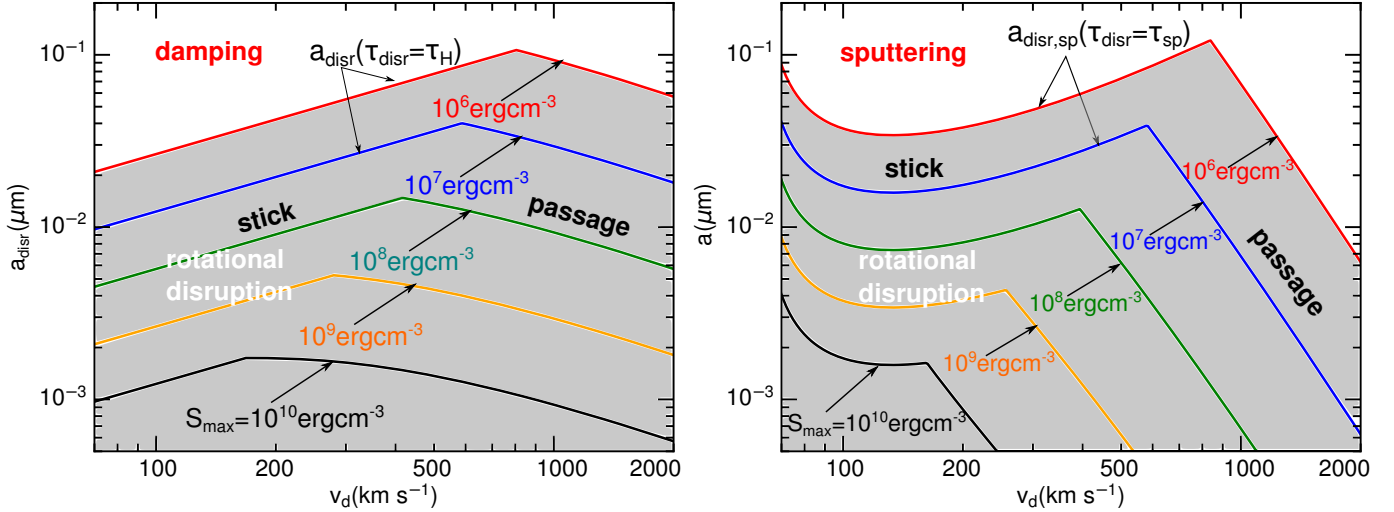


Figure 5. Grain disruption size vs. grain velocity assuming the different tensile strength of grain material. The solid lines mark the boundary between rotational disruption and damping ($\tau_{\text{disr}} = \tau_{\text{H}}$) and $\tau_{\text{disr}} = \tau_{\text{sp}}$ (right panel). Shaded areas mark the parameter space where rotational disruption (METD) is faster than rotational damping (left panel) and nonthermal sputtering (right panel).

4.2. Destruction of grains accelerated by radiation pressure and implications for IGM

Dust grains can be accelerated to hypersonic velocities by radiation pressure from intense radiation sources such as massive OB stars, supernovae (SNe), and Active Galactic Nuclei (see, e.g., Hoang 2017).

The maximum gas column density that a small grain of size $a < a_{\text{disr}}$ can traverse before being disrupted by rotational disruption is estimated as

$$N_{\text{max,disr}} = n_{\text{H}} v_d \tau_{\text{disr}} \simeq 1.5 \times 10^{18} a_{-6}^4 S_{\text{max},9} v_2^{-2} f_p^{-2} \text{ cm}^{-2}. \quad (48)$$

Similarly, one can evaluate the maximum distance determined by sputtering as

$$N_{\text{max,sp}} = n_{\text{H}} v_d \tau_{\text{sp}} \simeq 7.6 \times 10^{18} a_{-6} Y_{\text{sp},-1} \text{ cm}^{-2}, \quad (49)$$

where $Y_{\text{sp},-1} = Y_{\text{sp}}/(0.1)$.

The grain can only traverse a distance of $D_{\text{max,disr}} = N_{\text{max,disr}}/n_{\text{H}} \sim 10^4 (50/n_1) S_{\text{max},9} a_{-6}^4 v_2^{-2}$ AU before being disrupted by METD. However, if small grains can move at extreme speeds of $v_d > 1000 \text{ km s}^{-1}$, the effect of METD becomes less efficient due to the decrease of ion momentum transfer to the grain (i.e., $f_p \ll 1$).

Observations show the presence of dust in the circumgalactic medium (CGM) and intergalactic medium (IGM). The underlying mechanism to the existence of dust in the CGM and IGM is due to radiation pressure that expels grains at high speeds. The enrichment of metals and dust in the IGM is believed to arise from two main routes, including galactic winds driven by supernovae and the injection of galactic grains moving at

high velocities of $v_d > 100 \text{ km s}^{-1}$ accelerated by radiation pressure (see e.g., Bianchi & Ferrara 2005). Ferrara et al. (1991) find that radiation pressure from starlight can accelerate grains to $v_d \sim 100 - 600 \text{ km s}^{-1}$ from the Galaxy to galactic halo over a timescale of Myr. At such high velocities, our results show that small grains of sizes $a < 0.01 \mu\text{m}$ are efficiently destroyed by METD (see Figure 5, right panel) if they have non-ideal structures (i.e., composite or porous structures).

4.3. Mechanical torque disruption of dust grains in fast shocks

Shocks are ubiquitous in the interstellar medium, which includes slow shocks of velocities $v_{\text{sh}} < 50 \text{ km s}^{-1}$ driven by the outflow of young stars, stellar winds, and jets, and fast shocks of velocities $v_{\text{sh}} > 100 \text{ km s}^{-1}$ driven by supernova blast waves.

Grain shattering dominates for slow shocks (Draine & Salpeter 1979a; see Draine 1995), but for fast shocks, sputtering is dominant in destroying refractory grains of small sizes (Tielens et al. 1994).

A new understanding of dust destruction in shocks is presented in Hoang & Tram (2019) and Tram & Hoang (2019). For steady-state shocks, Hoang & Tram (2019), for the first time, found that nanoparticles of size $a < 2 \text{ nm}$ can be disrupted into molecules by mechanical torques due to stochastic gas bombardment (i.e., METD mechanism). For the same grain size, sputtering is found to have a lower destruction rate. In this paper, we found that rotational disruption is dominant over sputtering for fast shocks if grains are small or made of weak materials.

Fast shocks are very common in core-collapse supernova due to the interaction of ejecta with the surrounding environment (see e.g., Nozawa et al. 2006). Newly formed dust grains in the supernova ejecta are subject to reverse shocks and move at velocity of $2/(\gamma + 3)v_{\text{sh}}$ with adiabatic index $\gamma = 5/3$ relative to the gas (see e.g., Dwek et al. 1996; Bianchi & Schneider 2007). Traditionally, thermal and non-thermal sputtering is established to be a main destruction mechanism of dust, which controls the dust evolution in the early universe (Nozawa et al. 2006). Based on our present calculations, METD appears to dominate over sputtering for fast shocks (i.e., $v_{\text{sh}} > 100 \text{ km s}^{-1}$), especially for small grains with fluffy structures that have low tensile strength. Therefore, newly formed dust in supernova remnants (SNRs) is expected to have deficiency of small and very small grains of size $a < a_{\text{disr}}$ due to rotational disruption, which is in agreement with observations (see Micelotta et al. 2018 and reference therein).

Observational data by Williams et al. (2006) and Zhu et al. (2019) show that for the fraction of dust destroyed in fast shocks of core-collapse supernova is higher than theoretical predictions based on sputtering. The authors appeal to the porous structure of dust grains to enhance the sputtering rate. However, this observational puzzle can be explained by rotational disruption.

4.4. Rotational disruption cascade of small grains by gas bombardment

What is the subsequent evolution of fragments resulting from METD due to supersonic motion of grains through the gas? In the frame work of METD, resulting fragments can rotate at higher rotational rates than the original grain due to their smaller masses. As a result, they would be disrupted rapidly into smaller fragments. This results in collisional cascade of grains into smaller and smaller fragments. Finally, nonthermal sputtering acts to destroy such tiny fragments into individual atoms/molecules. The rotational disruption cascade is expected to begin with the RATD mechanism (Hoang et al. 2019) because small grains can survive against RATD due to their weaker radiative torques.

Finally, we note that, in this paper, spherical grains are considered and we disregarded the effect of regular mechanical torques acting on grains of irregular shapes (Lazarian & Hoang 2007; Das & Weingartner 2016; Hoang et al. 2018). The latter is expected to be more efficient.

4.5. Mechanical torque disruption in hot gas

In the post-shock regions or ionized plasma, gas can be heated to very high temperatures of $T_{\text{gas}} > 10^6 \text{ K}$. In

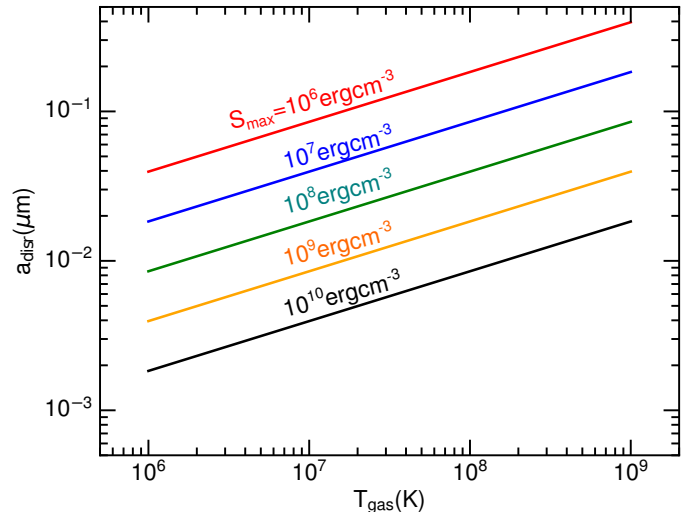


Figure 6. Grain disruption size as a function of the gas temperature in hot plasma assuming the different tensile strength.

such a hot gas, thermal collisions with protons can spin-up dust grains to extremely fast rotation with $\omega_{\text{rot}} = \omega_T$, resulting in the rotational disruption (Draine & Salpeter 1979b). Using the disruption criteria $\omega_{\text{rot}} = \omega_{\text{disr}}$, one obtains the disruption size for a given T_{gas} as follows:

$$a_{\text{disr}} = \left(\frac{45kT_{\text{gas}}}{32\pi S_{\text{max}}} \right)^{1/3} \simeq 0.02 S_{\text{max},9}^{-1/3} \left(\frac{T_{\text{gas}}}{10^8 \text{ K}} \right)^{1/3} \mu\text{m}, \quad (50)$$

The critical gas temperature required for rotational disruption in a hot plasma is given by

$$T_{\text{gas}} \gtrsim \left(\frac{32\pi a^3}{45k} \right) S_{\text{max}} \simeq 1.6 \times 10^7 a_{-6}^3 S_{\text{max},9} \text{ K}, \quad (51)$$

which implies that the rotational disruption is important for $T_{\text{gas}} \sim 10^6 \text{ K}$ if grains are as small as $0.01 \mu\text{m}$ and made of weak materials ($S_{\text{max}} < 10^9 \text{ erg cm}^{-3}$).

Figure 6 shows the disruption size as a function of the gas temperature. Small grains are destroyed by rotational disruption so that dust grains in hot plasma are only larger than a_{disr} . Large grains with weak structures can be destroyed by rotational disruption for temperatures $T_{\text{gas}} \sim 10^9 \text{ K}$. So, we predict that dust grains in very hot gas likely have a compact structure of high tensile strength.

5. SUMMARY

We study rotational disruption of dust grains by stochastic mechanical torques due to gas-grain collisions at high velocities. Our results are summarized as follows:

1. We find that very small and small grains can be disrupted by centrifugal stress within rapidly

- spinning grains due to stochastic gas-grain collisions when the relative grain velocity is sufficiently large. The exact velocity threshold for disruption is determined by the tensile strength of dust grains.
2. We compare the timescale of METD with sputtering timescale and find that rotational disruption is much more efficient than sputtering for grain velocities $v_d < 500 \text{ km s}^{-1}$. The ratio of rotational disruption to sputtering time is $\tau_{\text{disr}}/\tau_{\text{sp}} \sim 0.7 S_{\text{max},9} Y_{\text{sp},-1} a_{-6}^3 (\bar{A}_{\text{sp}}/12) (300 \text{ km s}^{-1}/v_d)^{-2}$. The internal structure of grains which determines the tensile strength is found to play a critical role in grain destruction by gas-grain collisions.
 3. At very high velocities (e.g., $v_d > 500 \text{ km s}^{-1}$), we find that the rate of METD for small grains is reduced by a factor f_p^2 because incident particles pass through the grain and transfer only a fraction f_p of their momentum to the grain.
 4. We discuss the implications of our study for the origin of intergalactic dust and find that small grains are likely disrupted before injecting into the IGM. Large grains of $a \sim 0.05 - 0.1 \mu\text{m}$ of weak material may be disrupted, but grains of strong

material such as compact grains can survive and reach the IGM.

5. Our results demonstrate that METD may be a dominant destruction mechanism of small grains in fast shocks of $v_{\text{sh}} > 100 \text{ km s}^{-1}$, instead of non-thermal sputtering as previously thought. Very small grains can be disrupted at lower velocities. This enhanced dust destruction rate appears to be consistent with dust destruction measured from fast shocks of core-collapse supernovae.
6. We also find that METD can also be more efficient than thermal sputtering for small grains of weak material in hot gas, assuming that grains rotate at thermal angular velocity.

ACKNOWLEDGMENTS

We are grateful to the referee, Dr. Joseph Nuth, for a constructive review that improves our manuscript. We thank A. Lazarian for his warm encouragements and Sergio M. Gonzalez for helpful comments. This work was supported by the National Research Foundation of Korea (NRF) grants funded by the Korea government (MSIT) through the Basic Science Research Program (2017R1D1A1B03035359) and Mid-career Research Program (2019R1A2C1087045).

REFERENCES

- Aguirre, A., Hernquist, L., Katz, N., Gardner, J., & Weinberg, D. 2001a, *ApJ*, 556, L11
- Aguirre, A., Hernquist, L., Schaye, J., et al. 2001b, *ApJ*, 561, 521
- Bianchi, S., & Ferrara, A. 2005, *MNRAS*, 358, 379
- Bianchi, S., & Schneider, R. 2007, *MNRAS*, 378, 973
- Bohdansky, J. 1984, *NIMPB*, 2, 587
- Das, I., & Weingartner, J. C. 2016, *MNRAS*, 457, 1958
- Dominik, C., & Tielens, A. G. G. M. 1997, *ApJ*, 480, 647
- Draine, B. T. 1995, *Astrophysics and Space Science*, 233, 111
- Draine, B. T., & Lazarian, A. 1998, *ApJ*, 508, 157
- Draine, B. T., & Salpeter, E. E. 1979a, *ApJ*, 231, 438
- Draine, B. T., & Salpeter, E. E. 1979b, *ApJ*, 231, 77
- Dwek, E., Foster, S. M., & Vancura, O. 1996, *ApJ*, 457, 244
- Ellison, D. C., Drury, L. O., & Meyer, J.-P. 1997, *ApJ*, 487, 197
- Epstein, R. I. 1980, *MNRAS*, 193, 723
- Ferrara, A., Ferrini, F., Franco, J., & Barsella, B. 1991, *Astrophysical Journal*, 381, 137
- Gold, T. 1952, *MNRAS*, 112, 215
- Goldreich, P., & Scoville, N. 1976, *ApJ*, 205, 144
- Guillet, V., Fanciullo, L., Verstraete, L., et al. 2017, *A&A*
- Hoang, T. 2017, *ApJ*, 847, 77
- Hoang, T. 2019, *ApJ*, 876, 13
- Hoang, T., Cho, J., & Lazarian, A. 2018, *ApJ*, 852, 129
- Hoang, T., Draine, B. T., & Lazarian, A. 2010, *ApJ*, 715, 1462
- Hoang, T., Lazarian, A., & Schlickeiser, R. 2012, *ApJ*, 747, 54
- Hoang, T., Lazarian, A., & Schlickeiser, R. 2015, *ApJ*, 806, 255
- Hoang, T., & Tram, L. N. 2019, *ApJ*, 877, 36
- Hoang, T., Tram, L. N., Lee, H., & Ahn, S.-H. 2019, *Nature Astronomy*, 3, 766
- Hoang, T., Vinh, N. A., & Quynh Lan, N. 2016, *ApJ*, 824, 18
- Ishibashi, W., & Fabian, A. C. 2015, *MNRAS*, 451, 93
- Jones, A. P., Tielens, A. G. G. M., Hollenbach, D. J., & McKee, C. F. 1994, *ApJ*, 433, 797
- Lakićević, M., van Loon, J. T., Meixner, M., et al. 2015, *ApJ*, 799, 50

- Lazarian, A., & Hoang, T. 2007, *ApJ*, 669, L77
- Micelotta, E. R., Matsuura, M., & Sarangi, A. 2018, *Space Sci Rev*, 1
- Netzer, N., & Elitzur, M. 1993, *ApJ*, 410, 701
- Nozawa, T., Kozasa, T., & Habe, A. 2006, *ApJ*, 648, 435
- Purcell, E. M., & Spitzer, L. J. 1971, *ApJ*, 167, 31
- Sankrit, R., Williams, B. J., Borkowski, K. J., et al. 2010, *ApJ*, 712, 1092
- Sigmund, P. 1981, in *Sputtering by Particle Bombardment I*, ed. R. Behrisch (New York: Springer), 9
- Silvia, D. W., Smith, B. D., & Shull, J. M. 2010, *ApJ*, 715, 1575
- Tielens, A. G. G. M., McKee, C. F., Seab, C. G., & Hollenbach, D. J. 1994, *ApJ*, 431, 321
- Tram, L. N., & Hoang, T. 2019, *ApJ*, 886, 44
- Williams, B. J., Borkowski, K. J., Reynolds, S. P., et al. 2006, *ApJ*, 652, L33
- Yan, H., Lazarian, A., & Draine, B. T. 2004, *ApJ*, 616, 895
- Zhu, H., Slane, P., Raymond, J., & Tian, W. W. 2019, arXiv:1907.06213, arXiv:1907.06213

APPENDIX

A. VALIDITY OF THE SLAB APPROXIMATION FOR THE MOMENTUM TRANSFER

In Section 2, we assumed a slab approximation to calculate the fraction of the momentum transfer of projectiles to the grain by high-energy collisions. Subsequently, the stochastic torques are calculated as in the case of low-energy collisions.

We now consider whether this assumption is valid. Let us consider an energetic ion bombarding the spherical grain surface at position described by polar angle θ . The ion energy transferred to the grain is in general given by

$$\delta E(\theta) = (2a \sin \theta) n S(E), \quad (\text{A1})$$

where the pathlength of the projectile in the grain is $2a \sin \theta$.

The corrected fraction of the momentum transfer to the grain is then equal to

$$f_{p,\text{corr}}(E, a) \equiv \frac{\delta p}{p} = \frac{\delta E}{2E} = \frac{a \sin \theta}{E} n S(E) = \left(\frac{3 \sin \theta}{2} \right) f_p(E, a), \quad (\text{A2})$$

where $f_p(E, a) = (2a/3E)nS(E)$ is the momentum transfer obtained from the slab approximation (see Equation (26)).

The increase in the squared angular momentum becomes

$$(\delta J)^2 = (a \cos \theta \delta p)^2 = (a \cos \theta p f_{p,\text{corr}})^2 = \frac{9a^2 p^2 \sin^2 \theta \cos^2 \theta}{4} f_p(E, a)^2 = \frac{9a^2 p^2 \sin^2(2\theta)}{8} f_p(E, a)^2. \quad (\text{A3})$$

By averaging the above equation over the grain surface (angle θ from $0 - \pi$), one obtains

$$\langle (\delta J)^2 \rangle = \left(\frac{a^2 p^2}{2} \right) f_p(E, a) \times \left(\frac{9}{8} \right). \quad (\text{A4})$$

Comparing Equation (A4) with (28) one can see that the exact calculation is larger than the slab approximation by a small factor of 9/8.